

Cell Death by Gallotannin Is Associated with Inhibition of the JAK/STAT Pathway in Human Colon Cancer Cells

Marwa Houssein, PhD^{1,2,†}, Widian Abi Saab, PhD^{3,4,†}, Mahmoud Khalil, PhD¹, Hala Khalife, PhD⁵, Maamoun Fatfat, PhD^{2,*}

¹ Department of Biological Sciences, Faculty of Science, Beirut Arab University, Beirut, Lebanon

² Center for Drug Discovery, American University of Beirut, Beirut, Lebanon

³ Department of Biology, American University of Beirut, Lebanon

⁴ Department of Biology College of Arts and Sciences, Albert Einstein College of Medicine United State, San Diego, California, United State

⁵ Rammal Laboratory (ATAC), Faculty of Sciences I, Lebanese University Hadath, Beirut, Lebanon

ARTICLE INFO

Article history:

Received 25 February 2020

Accepted 8 June 2020

Key words:

Apoptosis
caspase
colon cancer
gallotannin
JAK/STAT
senescence

ABSTRACT

Background: Gallotannin (GT) is a polyphenol that possesses interesting anticancer properties. However, the mechanisms underlying its antitumor effects have not been well defined.

Objective: This study was designed to clarify the mechanisms underlying GT antitumor effects in colon cancer cell lines.

Methods: Three isogenic HCT116 cell lines (p53^{+/+}, p53^{-/-}, and p21^{-/-}) were treated with GT for different time points then Western blot, flow cytometry, and senescence analysis were performed to examine the effect of GT on Mitogen-activated protein kinase (MAPK) and Janus kinase (JAK)/signal transducer and activator of transcription (STAT) effectors, STAT3 downstream apoptotic targets, Sub-G1 phase, and programmed cell death induction. Transfection using Invitrogen Lipofectamine 2000 Transfection Reagent (Thermo Fisher Scientific, Waltham, Massachusetts) were used to identify the role of p53 and p21 in the p53^{-/-} and p21^{-/-} cell lines.

Results: Both low and high GT concentrations caused MAPKs activation marked by upregulation of extracellular signal-regulated kinase (p-ERK). The preincubation with the antioxidant Tiron (Sigma-Aldrich, St Louis, Missouri) showed that GT's antitumor effects were not mediated by reactive oxygen species. We then examined the effect of GT on the JAK/STAT pathway, which is known to be activated in colorectal cancer. GT totally inhibited the JAK/STAT pathway effectors JAK2, STAT1, and STAT3 and their downstream apoptotic regulators B-cell lymphoma-extra large (Bcl-x_L) and c-Myc in all 3 cell lines. HCT116 cancer cells exhibited differential sensitivity to GT with p21^{-/-} cells being the most sensitive and p53^{+/+} cells that express p21 protein being the least sensitive. In p53^{+/+} cells, GT induced senescence, whereas in p53^{-/-} and p21^{-/-} cells, GT induced apoptosis in a caspase independent manner marked by Poly(ADP-Ribose) Polymerase (PARP) cleavage, Bcl-2 downregulation, and upregulation of the Bcl-2 associated X (Bax) to B-cell lymphoma 2 (Bcl-2) ratio. In addition, the sub-G1 phase exceeded 50% in p21^{-/-} cells.

Conclusions: Considered together, our results indicate that GT is potent inhibitor of the JAK/STAT pathway in colon cancer irrespective of the p53 and p21 status, which provides insights into its mechanism of anticancer activities and future potential for clinical translation. (*Curr Ther Res Clin Exp.* 2020; 81:XXX-XXX)

© 2020 The Authors. Published by Elsevier Inc.

This is an open access article under the CC BY-NC-ND license.

(<http://creativecommons.org/licenses/by-nc-nd/4.0/>)

* Address correspondence to: Mamoun Fatfat, PhD, Center for Drug Discovery, American University of Beirut, Riad El Solh, Beirut, Lebanon

E-mail address: Mf53@aub.edu.lb (M. Fatfat).

† These authors contributed equally to this work.

Introduction

Colorectal cancer is the third most commonly occurring cancer in men and the second in women. According to Global Cancer Incidence, Mortality and Prevalence (GLOBOCAN) 2018 data, 1,849,518 new cases of colorectal cancer were diagnosed worldwide with 1,026,215 new cases in men and 823,303 in women. The mortality

rate was about 880,792 with 484,224 deaths in men and 396,568 deaths in women.¹ The incidence of colorectal cancer increased among adults younger than age 50 years. This increase has been associated with an unfavorable diet and the prevalence of obesity.²

Colorectal cancer is initiated by alterations of 1 or more essential genes such as the tumor suppressor gene, adenomatous polyposis coli gene or *APC*, leading to the formation of aberrant crypt foci. Acquiring further molecular alterations allows these foci to progress into adenomas. At this stage the tumor is still benign, but additional genetic and/or epigenetic defects will lead to malignant transformation that upon further alterations in key genes, such as the tumor suppressor protein p53, the tumor will gain invasive potential.³ Colorectal cancer bears multiple genetic aberrations that render it resistant to therapy.⁴ For instance, the signal transducer and activator of transcription 3 (*STAT3*) was found to be constitutively activated in colorectal cancer.⁵ Moreover, in many cases, late colorectal cancers are characterized by the accumulation of β -catenin in the nucleus where it enhances the expression of several prosurvival genes, including *c-Myc* and *c-Jun*.⁶ During the past few years, despite advancements in cancer therapy, the response rates in advanced stages of colorectal cancer did not increase to more than 50% and the median survival of patients to more than 5 years.⁷

Natural products are source of numerous drugs and are the origin of about 35% of medicines. At the preclinical stage, many were tested and showed promising results against cancer such as resistin and bitter melon. Resistin, a proinflammatory cytokine, caused G1 arrest in colon cancer cells through upregulation of SOCS3.⁸ Bitter melon induced autophagy in colorectal and breast cancer cells⁹ and enhanced the natural killer mediated toxicity against head and neck cancer cells.^{10,11}

Polyphenols, which are plant secondary metabolites found in fruits, vegetables, and some of their derived products tea and wine, have been shown to have anti-colon cancer effects.¹² Gallotannin (GT), an hydrolyzable tannin, can be found in a variety of plants such as Chinese rose, Chinese gall, mango, and sumac among others and can be extracted from dried, fresh, or frozen plant sources. HPLC, column chromatography, and high-speed counter-current chromatography can recover GT with a level of purity of 99%.¹³ GT was previously shown to act as an anticancer agent in colon cancer by inhibiting 1, 2-dimethylhydrazine-induced colonic aberrant crypt foci and tumors.¹⁴ GT was also reported to induce cell senescence and apoptosis in colorectal carcinoma p53^{+/+} HCT116 and p53^{-/-} HCT116 cell lines, respectively, associated with reactive oxygen species (ROS) generation.¹⁵ Nevertheless, many aspects of the molecular mechanisms underlying the anti-colon cancer properties of GT remain elusive.

We investigated some of the molecular mechanisms underlying GT anticancer effect using 3 isogenic colon cancer cell lines, HCT116 p53^{+/+}, p53^{-/-}, and p21^{-/-}. GT inhibited JAK/STAT pathway in the different cell lines irrespective to their p53 or p21 status. Whereas HCT116 p53^{+/+} undergoes senescence upon GT treatment, a caspase-independent apoptotic response was detected in HCT116 p53^{-/-} and p21^{-/-} marked by PARP cleavage, downregulation of Bcl-2, and upregulation of Bax.

Materials and Methods

Cell culture and GT treatment

HCT116 (p53^{-/-}) and HCT116 (p21^{-/-}) cells were grown in Dulbecco's Modified Eagle Medium (Sigma-Aldrich, Munich, German) supplemented with sodium pyruvate and 4500 mg/L glucose. Roswell Park Memorial Institute (RPMI) 1640 with 25 mM N-2-hydroxyethylpiperazine-N-ethanesulfonic acid (HEPES) and L-glutamine was used as a medium for HCT116 (p53^{+/+}) human

colon cancer cells. One percent penicillin-streptomycin (100 U/mL) and 10% heat-inactivated foetal bovine serum (FBS) were added to all cell media. All culture cells were grown in a humidified atmosphere of 5% carbon dioxide and 95% air.

A stock of 10 mg GT (Sigma-Aldrich) was dissolved in 50 μ L 70% ice-cold ethanol and, depending on the cell type, 950 μ L either Dulbecco's Modified Eagle Medium or RPMI. The cells were treated with different drug concentrations (0–60 μ g/mL). Depending on the experiment done, the 3 cell lines were plated in 100 mm, 60 mm, 6-well, or 96-well plates at a plating density of 10⁵ for senescence and proliferation analyses or 1.2 \times 10⁵ cells/mL for proteins. At 50% confluency, the cells were treated and incubated with GT for 6, 15, 24, 48, or 72 hours. The HCT116 p53 null cells were kindly provided by Dr Carlos Galmarini, MD, PhD (INSERM, Lyon, France) and the HCT116 p53^{+/+} and p21^{-/-} were provided by Dr Regine Schneider-Stock, PhD (Erlangen, Germany).

Cell proliferation assay

The 3 isogenic HCT116 human colon cancer cells (p53^{+/+}, p53^{-/-}, and p21^{-/-}) cells were cultured at 10⁵ cells/mL in 96-well plates. After 24 hours, cells were treated in triplicates with 20 μ M caspase-3, caspase-8, caspase-9 inhibitors, or the universal caspase inhibitor for 1.5 hours followed with 20, 40, or 60 μ g/mL GT treatment. Proliferation effects were studied 48 hours post-treatment using the Cell Titer 96 (Promega Corporation, Madison, WI) nonradioactive cell proliferation kit.

The proliferation assay is a dye compound 3-(4,5-Dimethylthiazol-2-yl)-2,5-diphenyltetrazolium bromide for (MTT)-based method, which measures the ability of metabolically active cells to convert tetrazolium salt into a blue formazan product and the absorbance is recorded at 570 nm. In experiments that involved Tiron (Sigma-Aldrich, St Louis, Missouri), the cells were treated in triplicates with 1 or 2 mM Tiron for 1.5 hours followed by GT treatment.

Cell cycle analysis using flow cytometry

HCT116 (p21^{-/-}) cells were plated in 60-mm tissue culture dishes at a density of 1.2 \times 10⁵ cells/mL. At 50% confluency, cells were treated with different concentrations of GT and incubated for 48 hours. Cells were centrifuged at 4°C for 5 minutes at 1200 rpm. After that, pellets were washed by 1 \times phosphate buffered saline (PBS) then fixed with 70% ice-cold ethanol and stored at -20°C. After 24 hours, cells were washed with 1 \times PBS and incubated with 200 μ g/mL RNase for 1.5 hours at 37°C. A 6.25 μ g/mL propidium iodide was used for cells staining for at least 15 minutes. Fluorescence Activated Cell Sorter flow cytometer (Becton Dickinson, Research Triangle, NC) was used to measure the cellular fluorescence. Cell cycle analysis was then performed using the Cell Quest (BD Biosciences, USA) program and the percentages of cells distributed, according to their DNA content, were calculated. Cells in pre-G1 have DNA content <2n and represent apoptotic or necrotic cells.

Senescence analysis using the Senescence β -Galactosidase Staining Kit

HCT116 (p53^{+/+}, p53^{-/-}, and p21^{-/-}) cells were plated in 6-well plate at a density of 10⁵ cells/mL. Cells were treated with 20 or 40 μ g/mL GT and incubated for 72 hours at 50% confluency. At 72 hours, the growth medium was removed from the cells and the wells were washed with 2 mL 1 \times PBS. The cells in each well were then fixed with 1 mL 1 \times fixative solution provided by the Senescence β -Galactosidase Staining Kit (Sigma-Aldrich) for 15 minutes at room temperature. Cells were then washed twice with

2 mL $1 \times$ PBS. To each well, 1 mL staining solution mix containing 930 μ L staining solution, 10 μ L staining supplement A, 10 μ L staining supplement B, and 50 μ L 20 mg/mL X-gal dissolved in dimethylphenol was added. The cells were incubated overnight at 37°C. The next day, the development of blue color was detected under the microscope at 100 \times magnification. For quantification of senescent cells, 5 random regions were taken for each well and the percentage of senescing cells was calculated for each image.

TUNEL assay

To assess the induction of apoptosis by GT, fragmented DNA was detected by terminal deoxynucleotidyl transferase-mediated dUTP nick-end labeling (TUNEL assay; Roche Diagnostics, Basel, Switzerland). HCT116 (p21^{-/-}) cells were plated in 60-mm tissue culture dishes at a density of 105 cells/mL. The next day, cells were treated with different GT concentrations for 48 hours. Cells were then harvested and processed according to the manufacturer's instructions. The samples were examined by FACS can flow cytometer to determine the percentage of apoptotic cells in treated samples compared with the control samples.

Protein extraction and immunoblot analysis

HCT116 (p53^{+/+}, p53^{-/-}, and p21^{-/-}) cells were plated in 100-mm tissue culture dishes at a density of 1.2×10^5 cells/mL and treated with 40 μ g/mL GT for different durations. Cells were then washed with $1 \times$ PBS. This was followed by lysing and shearing steps. These steps were performed using a lysis buffer containing 50 mM Tris-HCl (pH 7.5), 150 mM sodium chloride, 1% Nonidet P40, 0.5% sodium deoxycholate, 4% protease inhibitors, and 1% phosphatase inhibitors. The cell lysates were centrifuged at 4°C for 30 minutes at a speed of 14,000 rpm and the pellets were discarded. Protein concentrations were quantified by the DC BioRad protein assay kit (BioRad Laboratories, Hercules, California) using bovine serum albumin as a standard. Protein samples were mixed with 10% β -mercaptoethanol and 2 \times sample buffer with bromophenol blue for gel electrophoresis.

Cellular proteins (40–80 μ g) were resolved by sodium dodecylsulphate-polyacrylamide gel electrophoresis on an 8%, 10%, 12%, or 15% denaturing polyacrylamide gel. The proteins were then transferred onto an activated polyvinylidene difluoride membrane in cold transfer buffer (14.4 g Glycine (BIO-RAD), 3 g Tris, and 1 g sodium dodecylsulphate dissolved in 20% methanol) at 30 volts overnight. After transfer, the membrane was blocked for 1 hour with 5% nonfat milk dissolved in Tris-buffered saline (TBS) containing 0.1% Tween-20 (BIO-RAD) and probed with primary antibodies diluted in 1% blocking buffer, either for 2 hours at room temperature or overnight at 4°C. The primary antibodies for PARP and JAK2 were diluted in 5% nonfat milk and the antibodies for p-STAT3 and p-STAT1 in 5% bovine serum albumin. All the antibodies were used at the dilution 1:1000. The membrane was then washed 3 times for 10 minutes each in $1 \times$ TBS containing 0.1% Tween 20 and incubated for 1 hour at room temperature in the appropriate secondary antibody. The membrane was again washed 3 times before protein detection by ECL (Santa-Cruz) chemiluminescence. The membrane was exposed to X-ray films (Hyperfilm ECL). Glyceraldehyde 3-phosphate dehydrogenase antibody was used as a loading control.

Transfection using Lipofectamine 2000

A measure of 8 μ g pCMV-p53 or pCMV-p53mt135 were diluted in 0.5 mL Opti-MEM I Reduced Serum Medium and mixed gently.

A measure of 20 μ L Lipofectamine 2000 (Thermo Fisher Scientific, Waltham, Massachusetts) was diluted in 0.5 mL Opti-MEM I (Thermo Fisher Scientific, Waltham, Massachusetts), Reduced Serum Medium. These were then mixed gently and incubated at room temperature for 5 minutes. After 5 minutes, the diluted DNA was combined with the diluted Lipofectamine 2000. The combination was then mixed gently and incubated for 20 minutes at room temperature to allow the DNA-Lipofectamine 2000 complexes to form. HCT116 (p53^{-/-}) cells were plated in 60-mm tissue culture plates in 5 mL growth medium without antibiotics at a density of 1.5×10^5 cells/mL. At 80% to 90% confluency, the growth medium was removed and 4 mL Opti-MEM I Reduced Serum Medium was added to each plate. One milliliter DNA-Lipofectamine 2000 complexes were then added to each plate. The cells were then incubated at 37°C in a carbon dioxide incubator for 30 hours and the transfection efficiency was about 80%. Transfected cells were then plated for subsequent senescence and Western blot analyses experiments. Backup plates were used to check for positive transfection by probing for p53 expression in these cells using Western blot analysis.

Results

Effect of GT on MAPK proteins

Considering that MAPK signaling pathway is implicated in the modulation of oxidative stress and in mediating the intracellular effects of ROS,¹⁶ we determined GT effects on p-ERK (Tyr 204), p-p38 (Tyr 182), and p-JNK (Thr 183, Tyr 185). In HCT116 (p53^{+/+}), a concentration of 40 μ g/mL GT led to an increase in p-ERK levels 15 hours posttreatment. However, the expression of this protein was transient and its levels started to decrease primarily 48 hours after treatment. The expression of p-p38 was not significantly changed at all time points. p-JNK levels, on the other hand, decreased in response to this GT concentration. MAPK protein levels were also modulated in HCT116 (p53^{-/-}) cells in response to 40 μ g/mL GT. p-ERK and p-JNK expression increased within 6 hours after treatment. The expression of these proteins was transient, attaining maximum increase at 15 hours, after which we observed a time-dependent decrease in their levels. The p-p38 protein expression levels were not modulated at all time points. In HCT116 (p21^{-/-}), p-JNK levels slightly decreased upon 40 μ g/mL GT treatment. At this GT concentration, p-ERK was significantly induced 6 hours after treatment. Moreover, a slight increase was detected in p-p38 15 hours posttreatment. The expression of both p-ERK and p-p38 was transient, and their levels decreased 24 hours after treatment (Fig. 1A).

The effect of 20 μ g/mL GT on the MAPK (p-p38, p-JNK, and p-ERK) proteins was also tested in the 3 cell lines. No changes in the expression levels of p-p38 and p-JNK were detected upon GT treatment. Nevertheless, GT significantly increased p-ERK proteins. This shows that activation of MAPKs, mainly p-ERK, is among the probable mechanisms by which GT mediates its oxidative effects (Fig. 1B).

ROS and GT-induced cell death

ROS in addition to its established role in promoting cell survival, can also trigger cell death and cell cycle arrest.¹⁷ To explore the role of ROS in GT-induced cell death, we preincubated cells with the ROS scavenger Tiron. HCT116 (p53^{+/+}, p53^{-/-}, and p21^{-/-}) cells were incubated with either 1 or 2 mM of Tiron before GT treatment and cell viability was assayed 48 hours posttreatment. In all cases, Tiron failed to rescue cells from GT-induced cell death. Rather, Tiron enhanced the antitumor effects of GT (Fig. 2A).

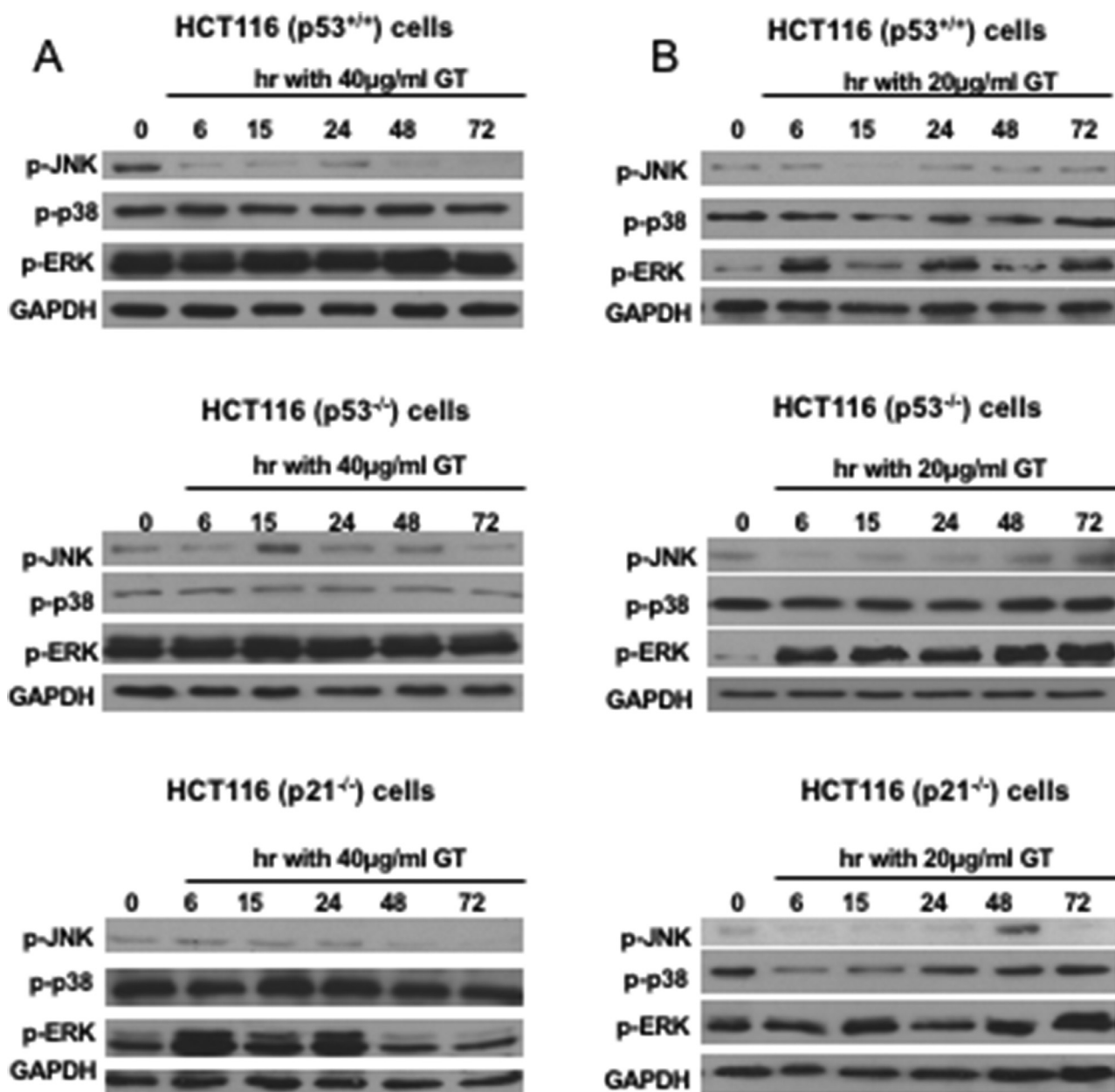


Fig. 1. (A) Treatment of HCT116 (p53^{+/+}, p53^{-/-}, and p21^{-/-}) cells with gallotannin (GT) did not significantly modulate the levels of MAPK proteins except for a slight increase in the levels of p-ERK (Tyr 204). In HCT116 (p53^{-/-}) cells p-JNK increased 15 hours posttreatment. The cells were treated at 50% confluency with 40 µg/mL GT for 6, 15, 24, 48, and 72 hours. Whole-cell lysates were then immunoblotted with p-ERK (Tyr 204), p-JNK (Thr 183, Tyr 185), and p-p38 (Tyr 182) antibodies. The membranes were also probed with glyceraldehyde 3-phosphate dehydrogenase (GAPDH) antibody to ensure equal loading. (B) Treatment of HCT116 (p53^{+/+}, p53^{-/-}, and p21^{-/-}) cells with GT increased the levels of p-ERK (Tyr 204) proteins. The cells were treated at 50% confluency with 20 µg/mL GT for 6, 15, 24, 48, and 72 hours. Whole-cell lysates were then immunoblotted with p-ERK (Tyr 204), p-JNK (Thr 183, Tyr 185), and p-p38 (Tyr 182) antibodies. The membranes were also probed with GAPDH antibody to ensure equal loading.

Effect of GT on JAK/STAT pathway and STAT3 downstream apoptotic regulators

We then examined the effect of GT on JAK/STAT pathway because STAT3 is constitutively activated in colon cancer and the inhibition of STAT3 expression has been shown to be accompanied by increased ROS levels¹⁸ and mitochondrial dysfunction.¹⁹ Previous studies showed that GT inhibits the viability of HCT116 (p53^{+/+}), HCT116 (p53^{-/-}), and HCT116 (p21^{-/-}) cells with IC₅₀ values of 45 µg/mL, 30 µg/mL, and 30 µg/mL, respectively.¹⁵ Here we show that the addition of 40 µg/mL GT caused a time-dependent decrease in the expression of both STAT3, STAT1, p-STAT1, and p-STAT3; JAK2 and p-JAK2

(Tyr1007/1008) in the 3 cell lines irrespective of their p53 or p21 status with maximum decrease being observed at 72 hours (Fig. 2B). This inhibition of STAT3 may explain the origin of ROS and the persistence of cell death even when using the antioxidant Tiron.

STAT1 and STAT3 have opposing effects; STAT1 is apoptotic and STAT3 is antiapoptotic.²⁰ However, both proteins were down-regulated in response to 40 µg/mL GT. To further understand the mechanism of this inhibition, we examined the effects of GT on downstream regulators of STAT3. Bcl-x_L and c-Myc are 2 downstream targets of STAT3 that possess antiapoptotic and proto-oncogenic functions, respectively.²¹ Thus, the expression patterns of these proteins in response to 40 µg/mL GT were studied. Bcl-x_L

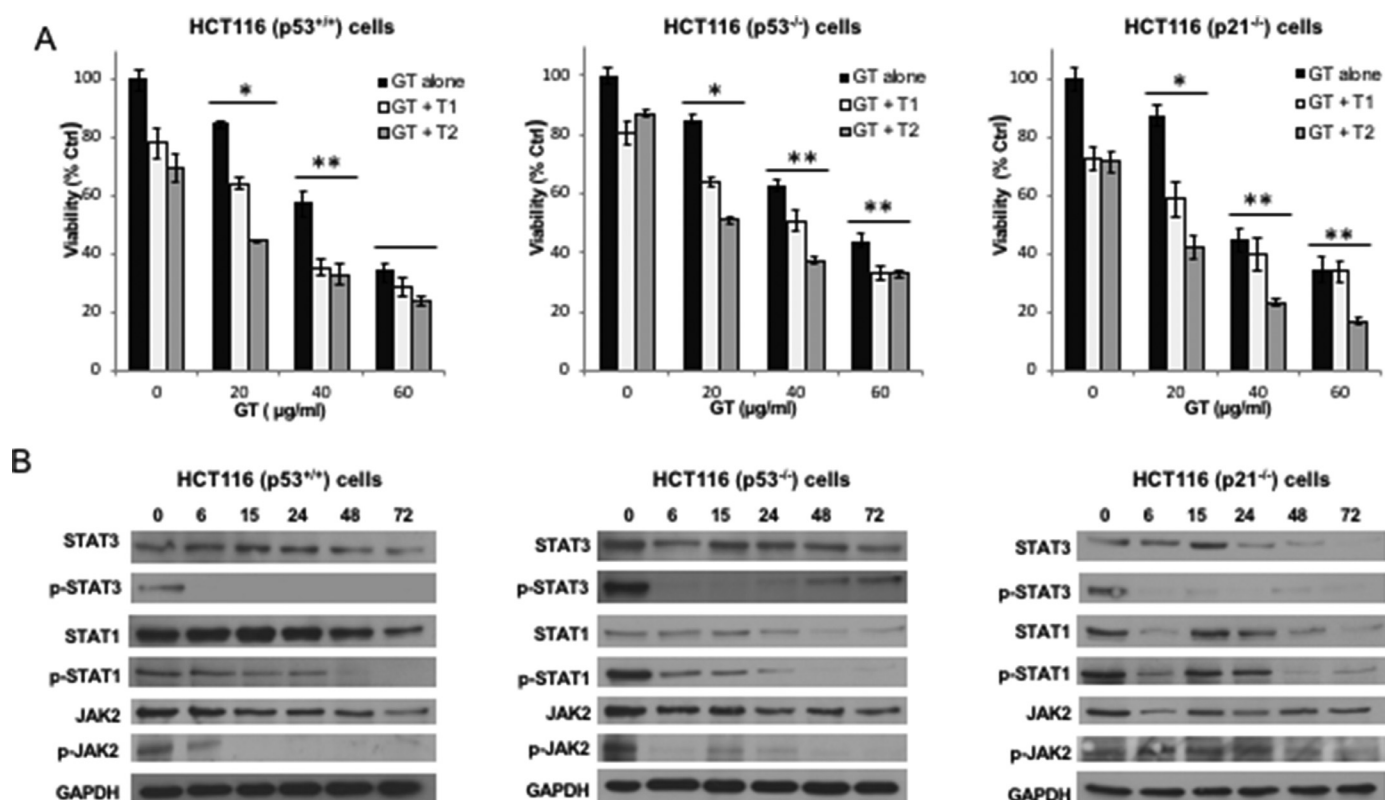


Fig. 2. (A) Gallotannin (GT) treatment reduces the proliferation of HCT116 (p53^{+/+}, p53^{-/-}, and p21^{-/-}) cells and Tiron addition does not counteract this antiproliferative activity. Cells were treated at 60% confluency with either 1 or 2 mM Tiron for 1.5 hours followed by addition of GT (20, 40, or 60 µg/mL) for 48 hours. Cell proliferation was determined by the Cell Titer96 nonradioactive cell proliferation assay as described in the Materials and Methods section. Each value is the mean (SD) of 3 separate experiments each done in triplicates. **P* < 0.05 and ***P* < 0.01 defined the statistical significance from control using 1-way ANOVA test. (B) Treatment of HCT-116 (p53^{+/+}, p53^{-/-}, and p21^{-/-}) cells with GT showed a decrease in the protein expression levels of STAT3, STAT1, p-STAT1 (Tyr 701), and p-STAT3 (Tyr 705) JAK2 as well as p-JAK2 (Tyr1007/1008). The cells were treated at 50% confluency with 40 µg/mL GT for 6, 15, 24, 48, and 72 hours. The membranes were also probed with glyceraldehyde 3-phosphate dehydrogenase (GAPDH) antibody to ensure equal loading. Whole-cell lysates were immunoblotted with STAT1 and STAT3, p-STAT1 (Tyr 701), p-STAT3 (Tyr 705), JAK2, and p-JAK2 (Tyr1007/1008) antibodies.

and c-Myc showed a time-dependent decrease in their expression levels compared with the control, in the 3 cell lines. This decrease was most evident at 72 hours of treatment in HCT116 (p53^{+/+}) and at 48 and 72 hours in p53^{-/-} and p21^{-/-} cells, respectively (Fig. 3A).

The antiapoptotic protein Bcl-2 is also a downstream target of STAT3. This protein blocks apoptosis by counteracting the effects of Bax.²² Therefore, whether apoptosis is executed or not depends on the ratio of Bax to Bcl-2 protein levels. As a result, possible modulation in the Bax/Bcl-2 ratio upon GT treatment was investigated. In HCT116 (p53^{+/+}), the Bax/Bcl-2 ratio was not significantly modulated. This ratio underwent a gradual increase starting 24 hours posttreatment, reaching about 2.9- and 4-fold increase in HCT116 (p53^{-/-}) and HCT116 (p21^{-/-}), respectively, and this increase was mainly due to an inhibition of Bcl-2 protein expression rather than an increase in Bax protein levels (Fig. 3B).

STAT3 is a negative regulator of mitochondrial-dependent cell death particularly caspase-dependent apoptosis.²³ Among the hallmarks of this type of death is PARP cleavage and inactivation. To determine whether the cell death effects of GT in HCT116 cell lines is mediated through the mitochondria, the expression levels of PARP and its cleaved product were monitored by Western blot analysis. No significant variation in the levels of full-length PARP was detected in the 3 cell lines, upon treatment with 40 µg/mL GT except for a major decrease in HCT116 (p21^{-/-}) cells 72 hours posttreatment. Nevertheless, the cleaved PARP (87 KDa) fragment was detected in the 3 cell lines starting 15 hours of treatment, indicating PARP cleavage. Cleaved PARP then exhibited a time-

dependent increase with maximum expression being observed at 72 hours (Fig. 3C).

Cell death and apoptotic effects of GT in HCT116 (p21^{-/-}) cells

Previous studies showed that GT caused S-phase arrest and cell death mainly through apoptosis in HCT116 (p53^{+/+}) cells and HCT116 (p53^{-/-}) cells, respectively, at 48 hours, at 40 or 60 µg/mL.¹⁵ To investigate the effects of GT on HCT116 (p21^{-/-}) cells, cells were treated with GT doses ranging from 20 to 60 µg/mL for 24 or 48 hours then harvested for flow cytometric analysis by propidium iodide staining. A concentration of 20 µg/mL GT caused only 2% increase in the sub-G₁ population. This percentage increased to 28.6% and 55.5% at concentrations of 40 and 60 µg/mL GT. To investigate the mode of cell death by GT, TUNEL assay was performed in HCT116 (p21^{-/-}) cell line and the results confirmed the induction of apoptosis by GT in this cell line (Fig. 4A).

Role of caspases in GT-induced cell death effects in p53^{-/-} and p21^{-/-} HCT116 cells

The caspase signaling cascade is the major pathway that leads to PARP cleavage and that elicits mitochondrial-dependent apoptosis.²⁴ Therefore, caspase involvement in GT-induced apoptosis was investigated in HCT116 (p53^{-/-}) and HCT116 (p21^{-/-}) cells by MTT assay using 20 µM of the different caspase inhibitors; namely caspase-3, -8, and -9 inhibitors and the universal caspase inhibitor

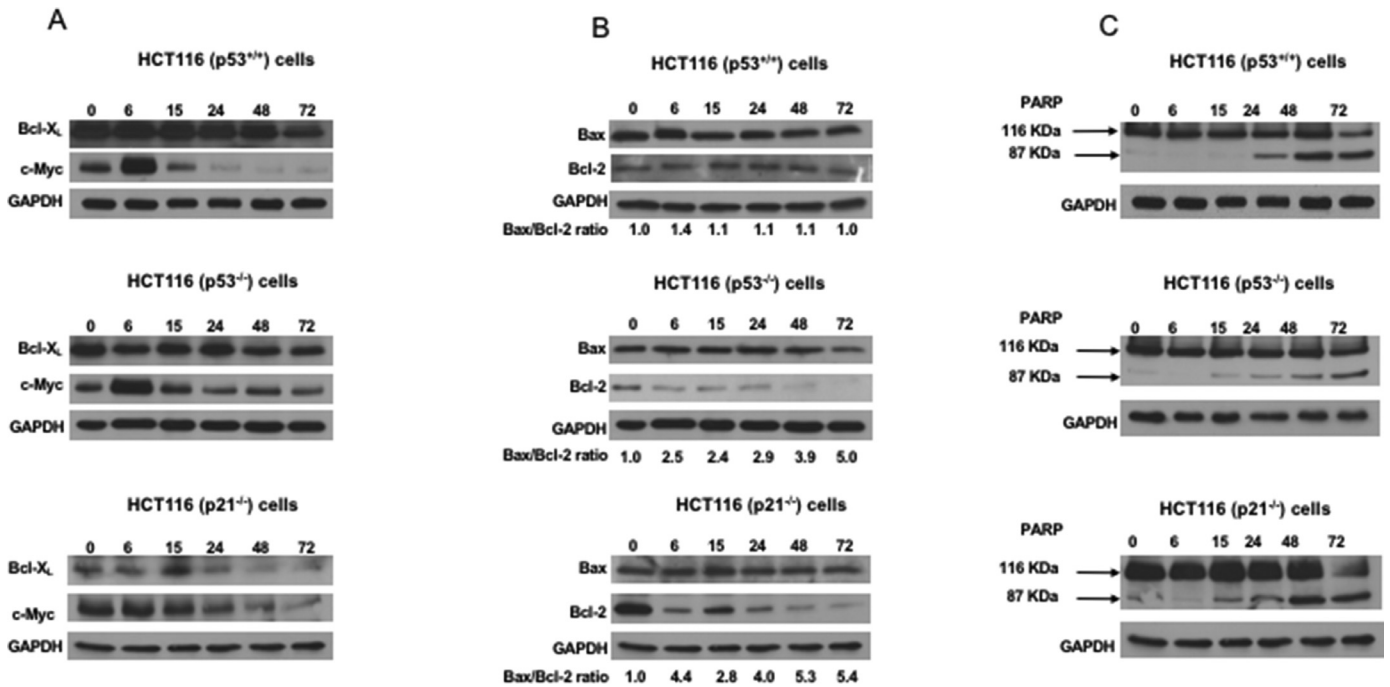


Fig. 3. Treatment of HCT116 (p53^{+/+}, p53^{-/-}, and p21^{-/-}) cells with gallotannin (GT) (A) downregulated the 2 anti-apoptotic proteins, Bcl-x_l and c-Myc; (B) did not modulate the Bax/Bcl-2 ratio in HCT116 (p53^{+/+}) cell line that is increased in HCT116 (p53^{-/-}) and (p21^{-/-}) cell line; and (C) induced PARP cleavage. The cells were treated at 50% confluency with 40 µg/mL GT for 6, 15, 24, 48, and 72 hours. Whole-cell lysates were then immunoblotted with specific antibody. The membranes were also probed with glyceraldehyde 3-phosphate dehydrogenase (GAPDH) antibody to ensure equal loading.

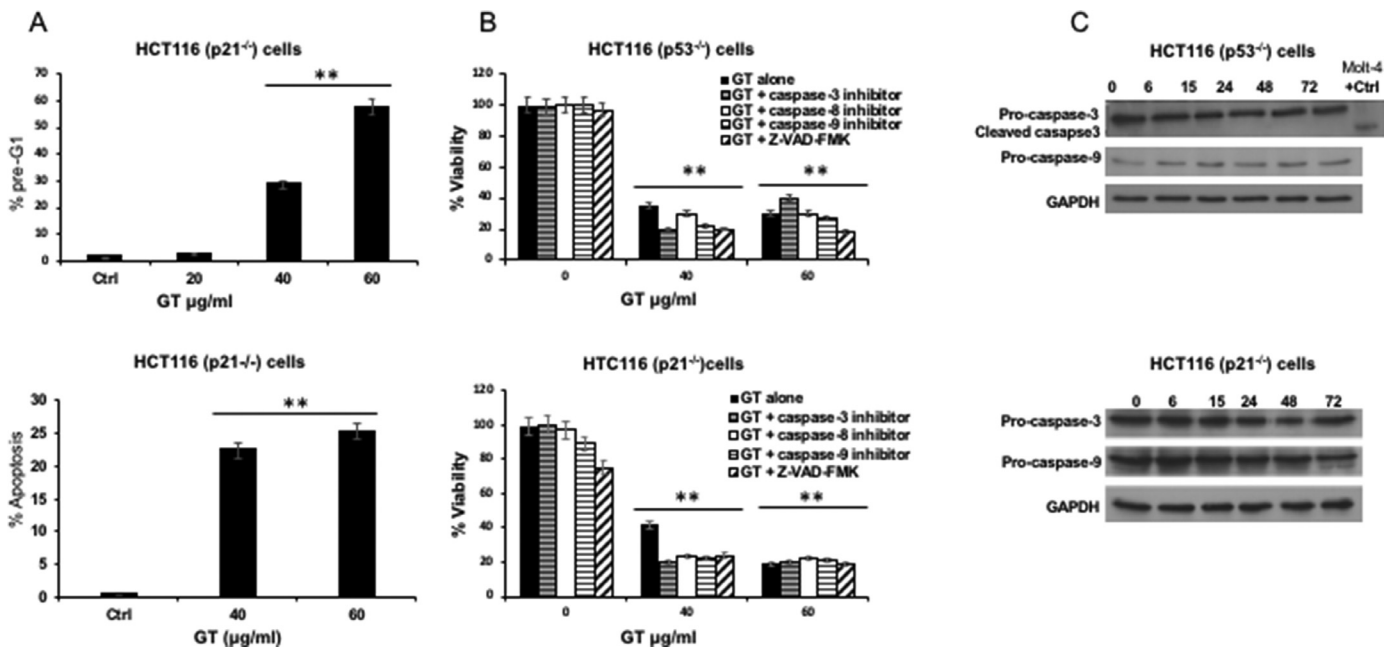


Fig. 4. (A) Treatment of HCT116 (p21^{-/-}) cells with gallotannin (GT) induced cell death as evidenced by the accumulation of cells in the subG0/G1 phase. Cells were treated at 50% confluency with GT (20, 40, and 60 µg/mL) for 48 hours. Cells were then harvested and DNA stained with propidium iodide (PI) for flow cytometric analysis of DNA content with FACScan flow cytometry. The percentage of cells in each of the cell cycle phases was calculated using Cell Quest. TUNEL assay (Roche Diagnostics, Basel, Switzerland) indicates that GT induced apoptosis in HCT-116 (p21^{-/-}) cells at 40 and 60 mg/mL 48 hours posttreatment. Cells were treated at 50% confluency with either <0.1% ethanol (control) or GT (40 or 60 mg/mL) for 48 hours. Cells were then harvested and DNA fragmentation was evaluated by TUNEL assay and reading by flow cytometry as described in the Materials and Methods section. The percentage of apoptotic cells under each treatment was obtained with Cell Quest. Each value is the mean of 2 separate experiments performed in triplicates. **P* < 0.05 and ***P* < 0.01 defined the statistical significance from control using 1-way ANOVA test. (B) GT treatment inhibits the proliferation of HCT116 (p53^{-/-}) and HCT116 (p21^{-/-}) cells, whereas concomitant treatment with the different caspase inhibitors had no effect on the antiproliferative effects of GT. Cells were treated at 50% confluency with 20 µM caspase inhibitors followed by addition of GT (0, 40, or 60 µg/mL) for 48 hours. Cell proliferation was determined by the Cell Titer 96 nonradioactive cell proliferation assay as described in the Materials and Methods section. Each value is the mean (SD) of 3 separate experiments each done in triplicates. **P* < 0.05 and ***P* < 0.01 defined the statistical significance from control using 1-way ANOVA test. (C) Treatment of HCT116 (p53^{-/-}) cells and HCT116 (p21^{-/-}) cells induced slight reduction in the levels of pro-caspase-3 and pro-caspase-9 protein levels; however, it failed to trigger caspase cleavage. The cleaved caspase product expressed by Molt-4 cells subjected to irradiation is used as positive control for pro-caspase-3 cleavage. The cells were treated at 50% confluency with 40 µg/mL GT for 6, 15, 24, 48, and 72 hours. Whole-cell lysates were then immunoblotted with caspase-3 and caspase-9 antibodies. The membranes were also probed with glyceraldehyde 3-phosphate dehydrogenase (GAPDH) antibody to ensure equal loading.

Z-VAD-fmk. The caspase inhibitors were added to the cells 1.5 hour before treatment with 40 $\mu\text{g}/\text{mL}$ GT and the samples were left for 48 hours. In the 2 cell lines, none of the above-mentioned caspase inhibitors were found to rescue cell death upon GT treatment, thus ruling out the possibility of caspase-dependent cell death (Fig. 4B).

To further corroborate our findings, alterations in the expression of 2 caspases; pro-caspase-3 and pro-caspase-9 and their cleaved and active forms were investigated. Pro-caspase-3 protein levels exhibited about 20% reduction in HCT116 ($p53^{-/-}$) cells and about 10% reduction in HCT116 ($p21^{-/-}$) cells. However, the cleaved product failed to appear in any of the treatments compared with total cleavage in positive control Molt-4 cells subjected to irradiation. Similarly, although pro-caspase-9 underwent a slight decrease in its expression upon GT treatment, this decrease was not associated with induction of the cleaved and active p10 fragment (Fig. 4C).

Role of p53 and p21 in GT-induced cell death effects

The 3 isogenic cell lines exhibited different sensitivities to GT, whereby HCT116 ($p53^{+/+}$) cells arrested at S phase and HCT116 ($p53^{-/-}$) and HCT116 ($p21^{-/-}$) cells underwent apoptosis. To investigate whether the observed cell cycle arrest in HCT116 ($p53^{+/+}$) is due to senescence and whether this effect depends on p21 expression, senescence induction in response to 20 and 40 $\mu\text{g}/\text{mL}$ GT was assayed in these cell lines 72 hours posttreatment by the Senescence β -Galactosidase Staining Kit. In HCT116 ($p53^{-/-}$ and $p21^{-/-}$), the percentage of senescent cells at both 20 and 40 $\mu\text{g}/\text{mL}$ GT were relatively comparable to that of the control and only ranged between 2% and 5%. However, in HCT116 ($p53^{+/+}$) cells, the percentage of senescent cells increased from 2.5% in the control to about 14% in response to 20 $\mu\text{g}/\text{mL}$ GT and to 12% in response to 40 $\mu\text{g}/\text{mL}$ GT (data not shown).

The role of p53 and p21 proteins in inducing senescence is well established. The p53-dependent senescence is mainly mediated by p21 that hypophosphorylates Retinoblastoma (p-Rb), increasing the levels of unphosphorylated and active Rb. Knowing that protein expression levels of p53 and p21 in HCT116 ($p53^{+/+}$), increase in a time-dependent manner in response to 40 $\mu\text{g}/\text{mL}$ GT, senescence induction in the 3 cell lines was further tested by monitoring changes in protein expression levels of p-Rb (Ser 780) and hypophosphorylated p-Rb or Rb. In HCT116 ($p21^{-/-}$), the levels of both p-Rb and Rb were not significantly modulated. In HCT116 ($p53^{-/-}$), although p-Rb expression decreased in a time-dependent manner, the protein levels of Rb did not vary much from the control. In contrast, p-Rb was almost totally inhibited 48 and 72 hours posttreatment in HCT116 ($p53^{+/+}$). This inhibition was associated with an increase in Rb protein levels at 24 and 48 hours (Fig. 4A).

To further confirm the role of p53 and p21 in senescence induction, HCT116 ($p53^{-/-}$) were transfected with either a plasmid encoding wild type p53 gene, pCMV-p53, or a plasmid encoding a p53 gene that harbors a G to A conversion at nucleotide 1017, pCMV-p53mt135. This gene encodes a dominant-negative mutation of p53, p53m that blocks normal p53 activity. Senescence induction in transfectants was also assayed using the Senescence β -Galactosidase Staining Kit. However, unexpectedly, senescence was not detected in either transfectant. The percentage of senescent cells upon treatment increased by only 2% to 5% at 20 and 40 $\mu\text{g}/\text{mL}$ GT in HCT116 ($p53^{-/-}$) cells transfected with p53mt and p53, respectively. These results were comparable to those of HCT116 ($p53^{-/-}$); however, were much less than those of HCT116 ($p53^{+/+}$) that exhibited 10% to 12% increase at these concentrations (Fig. 5B).

To explain the absence of senescence induction in HCT116 ($p53^{-/-}$) cells transfected with pCMV-p53, the protein level of p53

and p21 was assessed in the transfectants treated with 20 and 40 $\mu\text{g}/\text{mL}$ GT. In HCT116 ($p53^{-/-}$) cells transfected with pCMV-p53mt135, p53 proteins were poorly expressed in both treatments and at all time points. Similarly, p21 proteins were very poorly expressed in all cases (Fig. 5C). In HCT116 ($p53^{-/-}$) cells transfected with pCMV-p53, at 20 $\mu\text{g}/\text{mL}$ concentration, p53 protein levels 48 and 72 hours posttreatment were comparable to the respective controls. At 40 $\mu\text{g}/\text{mL}$ GT, p53 protein expression was significantly induced at 24 and 48 hours posttreatment compared with the controls. The p21 protein was very poorly expressed in these cells at 20 $\mu\text{g}/\text{mL}$ treatment. At 40 $\mu\text{g}/\text{mL}$ GT, the increase in p53 expression was not associated with p21 induction (Fig. 5D). These results confirm previous findings in which GT-induced senescence was found to be independent of p53 and p21.¹⁵

Discussion

GT is known to exert anticarcinogenic effects²⁵ on multiple cancer types, including prostate cancer and breast cancer, among others.²⁶ However, the mechanisms underlying this effect are not well defined. In colon cancer, GT was shown to induce cell death in HCT116 ($p53^{+/+}$, $p53^{-/-}$, and $p21^{-/-}$) cell lines that was associated with ROS generation.¹⁵ Moreover, the MAPK proteins that can be activated by ROS were not significantly modulated in response to GT, except for a relative increase in the expression levels of p-ERK. This could be explained by that this increase of p-ERK is mediated by ROS independent pathway.

The use of the ROS scavenger, Tiron, failed to rescue GT-induced cell death. The constitutive activation of STAT3 in colon cancer is well established. In addition, inhibition of STAT3 is known to increase ROS production on normal and cancer cells. To create a link between cell death, ROS, and GT; GT effects were tested on the JAK/STAT pathway. GT was found to completely abolish the phosphorylation of STAT3 at Y705 in the 3 isogenic human colon cancer cell lines HCT116 ($p53^{+/+}$, $p53^{-/-}$, and $p21^{-/-}$) at a concentration of 40 $\mu\text{g}/\text{mL}$. This GT concentration reduced the phosphorylation of STAT1 at Y701, and the protein expression levels of both STAT3 and STAT1. STAT3 possesses oncogenic potentials, thus promoting cell proliferation and survival.²⁷ STAT1, on the other hand, is apoptotic.²⁸ Despite reduction in p-STAT1 levels, GT most likely exerts its anticancer and apoptotic effects by inhibiting active STAT3, especially that this protein has been suggested to be a therapeutic target in many malignancies.²⁹ In our model system, STAT3 rather than STAT1 seems to be more important in determining cell fate, especially the effect of STAT3 on ROS production. GT also reduced JAK2 and totally blocked the phosphorylation of JAK2 at Y1007/1008. JAK2, which is part of the Janus kinases, is an upstream positive regulator of STAT3.³⁰ The JAK2/STAT3 pathway is mainly activated by interleukins (ILs), primary IL-6, and other gp130-related cytokines.³¹ Because the proliferation of colorectal cancer cells is promoted by IL-6,³² which ensures the activation of STAT3 in HCT116³³ and because GT inhibits p-STAT3 and reduces p-STAT1 levels even within 6 hours after treatment, GT could suppress the JAK/STAT pathway by blocking the association of IL-6 or other ILs to its corresponding receptor or by inhibiting JAK itself allowing the suppression of its downstream effectors. The JAK/STAT pathway also activates the transcription of STAT proteins. Therefore, the observed reduction in STAT3 and STAT1 levels could be due to GT-induced inhibition and reduction of p-STAT3 and p-STAT1, respectively, or due to the suppression of their corresponding JAKs. GT also downregulated the protein expression levels of the negative regulators of apoptosis (ie, Bcl-x_L, Bcl-2, and c-Myc) in the 3 cell lines.

In HCT116 ($p53^{-/-}$ and $p21^{-/-}$), apoptosis was induced in response to 40 $\mu\text{g}/\text{mL}$ GT as evidenced by the significant reduction

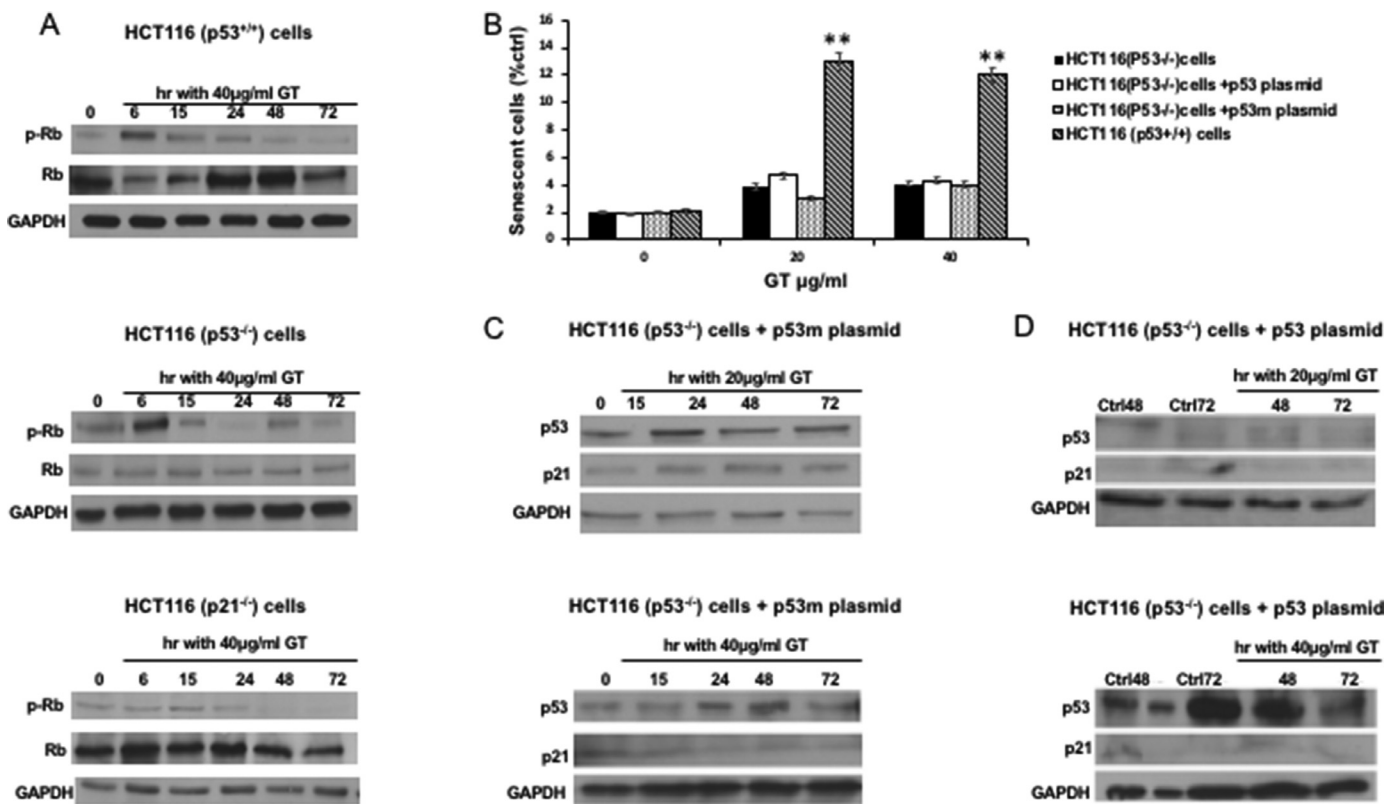


Fig. 5. (A) Treatment of HCT116 (p53^{+/+}) with gallotannin (GT) decreased p-Rb (Ser 780) expression and induced increase in Rb expression. Treatment of HCT116 (p53^{-/-} and p21^{-/-}) cells decreased the levels of p-Rb (Ser 780) but did not induce Rb expression. The cells were treated at 50% confluency with 40 µg/mL GT for 6, 15, 24, 48, and 72 hours. Whole-cell lysates were then immunoblotted with p-Rb (Ser 780) and Rb antibodies. The membranes were also probed with glyceraldehyde 3-phosphate dehydrogenase (GAPDH) antibody to ensure equal loading. (B) GT-induced senescence only in HCT116 (p53^{+/+}) cells but failed to induce it in HCT116 (p53^{-/-}) cells transfected with pCMV-p53 plasmid or pCMV-p53mt135 and in HCT116 (p53^{-/-}) cells. Cells were treated at 50% confluency with GT (20 and 40 µg/mL) for 72 hour. Senescence induction was assayed by the Senescence β -galactosidase Staining kit as described in the Materials and Methods section. Five random images were then taken for each sample and the percentage of stained cells was calculated in each image. The percentage of senescent cells in each sample represents the average of the percentages of stained cells in the 5 regions. ***P* < 0.01 defined the statistical significance from control using 1-way ANOVA test. (C, D) Treatment of HCT116 (p53^{-/-}) cells, transfected with p53 plasmid (pCMV-p53) or plasmid harboring p53 mutant p53m plasmid (pCMV-p53mt135) with 40 µg/mL GT induced significant p53 expression in cells transfected with pCMV-p53 plasmid but failed to express p21 proteins. In cells transfected with pCMV-p53mt135, p53 was slightly induced but not p21. Treatment of both types of transfected cells with 20 µg/mL GT failed to induce both p53 and p21 proteins. The cells were treated at 50% confluency with 20 or 40 µg/mL GT for 6, 15, 24, 48, or 72 hours. Whole-cell lysates were then immunoblotted with p53 and p21 antibodies. The membranes were also probed with GAPDH antibody to ensure equal loading.

in Bcl-2 protein levels which led to at least a 2-fold increase in the Bax/Bcl-2 ratio. Bcl-2 and Bcl-x_L normally block mitochondrial membrane potential and the subsequent membrane permeabilization and release of small apoptotic proteins such as cytochrome c and the apoptosis-inducing factor. Therefore, the decrease in Bcl-x_L and Bcl-2 protein expression levels upon GT treatment, and which could be attributed to inhibition of STAT3 phosphorylation, would relieve their suppressive effects on the mitochondria. This will then trigger mitochondrial-dependent apoptosis.

GT also induced significant PARP cleavage. PARP cleavage is mainly mediated by the caspase-signaling cascade. However, GT was found, using caspase inhibitors and Western blot analysis of essential caspases, to induce caspase-independent apoptosis. Thus, in our cell model, GT caused PARP cleavage in a caspase-independent manner. The mitochondrial protein apoptosis-inducing factor is the main protein that triggers caspase-independent apoptosis.³⁴ Thus, apoptosis in HCT116 (p53^{-/-} and p21^{-/-}) could be mediated by the apoptosis-inducing factor in a caspase-independent manner.

The proto-oncogene *c-myc* is another downstream target of STAT3 that is positively regulated by it.³⁵ The protein levels of c-Myc were reduced in response to GT's inhibitory effect on STAT3

phosphorylation. However, a marked increase in c-Myc expression was observed 6 hours posttreatment particularly in HCT116 (p53^{+/+}) and HCT116 (p53^{-/-}). This protein has been reported to elevate the intracellular levels of ROS. Knowing that GT induces ROS in these cell lines, c-Myc induction may at least partially contribute to this intracellular elevation in ROS.³⁶

The 3 cell lines used in this study display differential sensitivity to GT, with HCT116 (p53^{+/+}) being least sensitive and HCT116 (p21^{-/-}) most sensitive. This difference in response could be ascribed to the difference in the p53 and p21 status in the 3 cell lines. GT induced senescence in HCT116 (p53^{+/+}) cells with concomitant reduction in p-Rb (Ser 780) and induction of Rb levels. This cell line overexpresses p53 and p21 in response to GT. p21 activates Rb and once activated, Rb proteins associate with and block the activity of E2F proteins that are essential for S-phase progression.³⁷

Senescence is negatively modulated by STAT3. Senescence was induced in response to 2 GT concentrations 20 and 40 µg/mL. p-STAT3 inhibition was achieved at 40 µg/mL GT. Increase in intracellular ROS levels can induce senescence. GT was found to elevate the ROS levels in HCT116 (p53^{+/+}). The overall elevation in ROS generated from c-Myc induction, STAT3 inhibition and GT direct effect, can be partially involved in the senescence induction

in this cell line. Inhibition of STAT3 in HCT116 cell line have been reported to induce premature senescence.³⁸ This could explain senescence in HCT116 (p53^{+/+}) upon GT treatment when STAT3 inhibition is the main player in this induction.

The HCT116 (p21^{-/-}) that do not express p21 were most sensitive to GT, with the population of cells in the sub-G1 phase exceeding 50%. HCT116 (p53^{-/-}) also fail to express p21 and yet are more resistant to apoptosis. This difference in sensitivity could be ascribed to variations in the p53 status in the 2 cell lines. HCT116 (p21^{-/-}) express p53. This protein is mainly implicated in cell-cycle arrest by activating p21; however, its role in mediating mitochondrial-dependent apoptosis is also well established.³⁹ p53 can actually behave as the pro-apoptotic members of the Bcl-2 family and is also negatively regulated by STAT3.⁴⁰ Therefore, the increased sensitivity to GT in HCT116 (p21^{-/-}) cells could be due to activation of p53 following p-STAT3 inhibition. However, because the p21 gene is absent in these cells, p53 will mainly exert a pro-apoptotic effect, thus enhancing the apoptotic response to GT.

Conclusions

This study sheds light on the possible mode of action of GT in 3 isogenic human colon cancer cell lines. Based on our findings, particularly the p-STAT3 inhibitory effect, GT could be a promising chemotherapeutic agent. However, further studies need to be conducted to better understand the intracellular effects of GT. Studies regarding the modulation of IL-6 as well as the gp130 receptors would be necessary to understand the mechanism by which GT inhibits p-STAT3.

Acknowledgments

Marwa Houssein and Widian Abi Saab performed the whole experiments, literature search, figures creation, writing and data analysis. Mahmoud Khalil supervised Marwa Houssein. Hala Khalife helped in the data analysis and experimental setup. Maamoun Fatfat worked in the study design and data interpretation.

Conflicts of Interest

The authors have indicated that they have no conflicts of interest regarding the content of this article.

References

- Bray F, Ferlay J, Soerjomataram I, Siegel RL, Torre LA, Jemal A. Global cancer statistics 2018: GLOBOCAN estimates of incidence and mortality worldwide for 36 cancers in 185 countries. *CA: a cancer journal for clinicians*. 2018;68:394–424.
- Siegel R, Desantis C, Jemal A. Colorectal cancer statistics, 2014. *CA: a cancer journal for clinicians*. 2014;64:104–117.
- Umar A, Viner JL, Richmond E, Anderson WF, Hawk ET. Chemoprevention of colorectal carcinogenesis. *International journal of clinical oncology*. 2002;7:2–26.
- Deen KI, Silva H, Deen R, Chandrasinghe PC. Colorectal cancer in the young, many questions, few answers. *World journal of gastrointestinal oncology*. 2016;8:481–488.
- Tang S, Yuan X, Song J, Chen Y, Tan X, Li Q. Association analyses of the JAK/STAT signaling pathway with the progression and prognosis of colon cancer. *Oncology letters*. 2019;17:159–164.
- Shang S, Hua F, Hu ZW. The regulation of beta-catenin activity and function in cancer: therapeutic opportunities. *Oncotarget*. 2017;8:33972–33989.
- Bujanda L, Sarasqueta C, Hijona E, et al. Colorectal cancer prognosis twenty years later. *World journal of gastroenterology*. 2010;16:862–867.
- Singh S, Chouhan S, Mohammad N, Bhat MK. Resistin causes G1 arrest in colon cancer cells through upregulation of SOCS3. *FEBS letters*. 2017;591:1371–1382.
- Muhammad N, Steele R, Isbell TS, Philips N, Ray RB. Bitter melon extract inhibits breast cancer growth in preclinical model by inducing autophagic cell death. *Oncotarget*. 2017;8:66226–66236.
- Bhattacharya S, Muhammad N, Steele R, Kornbluth J, Ray RB. Bitter Melon Enhances Natural Killer-Mediated Toxicity against Head and Neck Cancer Cells. *Cancer prevention research (Philadelphia, Pa.)*. 2017;10:337–344.
- Bhattacharya S, Muhammad N, Steele R, Peng G, Ray RB. Immunomodulatory role of bitter melon extract in inhibition of head and neck squamous cell carcinoma growth. *Oncotarget*. 2016;7:33202–33209.
- Niedzwiecki A, Roomi MW, Kalinovsky T, Rath M. Anticancer Efficacy of Polyphenols and Their Combinations. *Nutrients*. 2016;8.
- Cristian Torres-León a JV-Sa, Lilianna Serna-Cock b, Juan A, Ascacio-Valdés a, Juan Contreras-Esquivel a CNA. Pentagalloylglucose (PGG): A valuable phenolic compound with functional properties. *Journal of Functional Foods*. 2017;37:176–189.
- Gali-Muhtasib HU, Younes IH, Karchesy JJ, el-Sabban ME. Plant tannins inhibit the induction of aberrant crypt foci and colonic tumors by 1,2-dimethylhydrazine in mice. *Nutrition and cancer*. 2001;39:108–116.
- Al-Ayyoubi S, Gali-Muhtasib H. Differential apoptosis by gallotannin in human colon cancer cells with distinct p53 status. *Molecular carcinogenesis*. 2007;46:176–186.
- Son Y, Kim S, Chung HT, Pae HO. Reactive oxygen species in the activation of MAP kinases. *Methods in enzymology*. 2013;528:27–48.
- Holze C, Michaudel C, Mackowiak C, et al. Oxeiptosis, a ROS-induced caspase-independent apoptosis-like cell-death pathway. *Nature immunology*. 2018;19:130–140.
- Liu X, Guo W, Wu S, et al. Antitumor activity of a novel STAT3 inhibitor and redox modulator in non-small cell lung cancer cells. *Biochemical pharmacology*. 2012;83:1456–1464.
- Du W, Hong J, Wang YC, et al. Inhibition of JAK2/STAT3 signalling induces colorectal cancer cell apoptosis via mitochondrial pathway. *Journal of cellular and molecular medicine*. 2012;16:1878–1888.
- Avalle L, Pensa S, Regis G, Novelli F, Poli V. STAT1 and STAT3 in tumorigenesis: A matter of balance. *Jak-stat*. 2012;1:65–72.
- Chong PSY, Chng WJ, de Mel S. STAT3: A Promising Therapeutic Target in Multiple Myeloma. *Cancers*. 2019:11.
- Naseri MH, Mahdavi M, Davoodi J, Tackallou SH, Goudarzvand M, Neishabouri SH. Up regulation of Bax and down regulation of Bcl2 during 3-NC mediated apoptosis in human cancer cells. *Cancer cell international*. 2015;15:55.
- Rincon M, Pereira FV. A New Perspective: Mitochondrial Stat3 as a Regulator for Lymphocyte Function. *International journal of molecular sciences*. 2018:19.
- Chaitanya GV, Steven AJ, Babu PP. PARP-1 cleavage fragments: signatures of cell-death proteases in neurodegeneration. *Cell communication and signaling: CCS*. 2010;8:31.
- Gali-Muhtasib H, Marwa H. Cell Death Mechanisms of the Promising Anticancer Compound Gallotannin. *IntechOpen*. 2019.
- Verma S, Singh A, Mishra A. Gallic acid: molecular rival of cancer. *Environmental toxicology and pharmacology*. 2013;35:473–485.
- Sellier H, Rébillard A, Guette C, Barré B, Coqueret O. How should we define STAT3 as an oncogene and as a potential target for therapy. *Jak-stat*. 2013;2:e24716.
- Zhang Y, Zhang Y, Yun H, Lai R, Su M. Correlation of STAT1 with apoptosis and cell-cycle markers in esophageal squamous cell carcinoma. *PLoS one*. 2014;9.
- Al Zaid Siddiquee K, Turkson J. STAT3 as a target for inducing apoptosis in solid and hematological tumors. *Cell research*. 2008;18:254–267.
- Villarino AV, Kanno Y, Ferdinand JR, O'Shea JJ. Mechanisms of Jak/STAT signaling in immunity and disease. *Journal of immunology (Baltimore, Md.: 1950)*. 2015;194:21–27.
- Sansone P, Bromberg J. Targeting the interleukin-6/Jak/stat pathway in human malignancies. *Journal of clinical oncology: official journal of the American Society of Clinical Oncology*. 2012;30:1005–1014.
- Waldner MJ, Foersch S, Neurath MF. Interleukin-6—a key regulator of colorectal cancer development. *International journal of biological sciences*. 2012;8:1248–1253.
- Shi W, Yan D, Zhao C, et al. Inhibition of IL-6/STAT3 signaling in human cancer cells using Evista. *Biochemical and biophysical research communications*. 2017;491:159–165.
- Candé C, Vahsen N, Garrido C, Kroemer G. Apoptosis-inducing factor (AIF): caspase-independent after all. *Cell death and differentiation*. 2004;11:591–595.
- Barré B, Vigneron A, Coqueret O. The STAT3 transcription factor is a target for the Myc and riboblastoma proteins on the Cdc25A promoter. *The Journal of biological chemistry*. 2005;280:15673–15681.
- Wu G, Liu T, Li H, Li Y, Li D, Li W. c-MYC and reactive oxygen species play roles in tetrandrine-induced leukemia differentiation. *Cell death & disease*. 2018;9:473.
- Johnson J, Thijssen B, McDermott U, Garnett M, Wessels LF, Bernards R. Targeting the RB-E2F pathway in breast cancer. *Oncogene*. 2016;35:4829–4835.
- Yun UJ, Park SE, Jo YS, Kim J, Shin DY. DNA damage induces the IL-6/STAT3 signaling pathway, which has anti-senescence and growth-promoting functions in human tumors. *Cancer letters*. 2012;323:155–160.
- Marchenko ND, Moll UM. Mitochondrial death functions of p53. *Molecular & cellular oncology*. 2014:1.
- Yu H, Yue X, Zhao Y, et al. LIF negatively regulates tumour-suppressor p53 through Stat3/ID1/MDM2 in colorectal cancers. *Nature communications*. 2014;5:5218.